Inorganic Chemistry
Article

Inorg. Chem. **2009**, *48*, 9853–9860 **9853**
DOI: 10.1021/ic901401t

Syntheses and Photophysical Behavior of Porphyrin Isomer Sn(IV) Complexes

Daisuke Maeda, Hisashi Shimakoshi, Masaaki Abe, and Yoshio Hisaeda*

Department of Chemistry and Biochemistry, Graduate School of Engineering, Kyushu University, Fukuoka 819-0395, Japan

Received July 17, 2009

2,3,6,7,12,13,16,17-Octaethylhemiporphycenato Sn(IV) chloride, [Sn^{IV}(OEHPc)Cl_2], and 2,3,6,7,12,13,16,17-octaethylporphycenato Sn(IV) chloride, [Sn^{IV}(OEPc)Cl_2], were synthesized in high yields and fully characterized by various spectroscopic methods. The X-ray crystal structures of the Sn(IV) complexes with porphycene and hemiporphycene were determined for the first time. The photophysical and photochemical properties of the singlet state of the Sn(IV) porphycene and hemiporphycene complexes, structural isomers of porphyrin, have been investigated by fluorescence and phosphorescence spectroscopies. The relatively strong emission and long fluorescence lifetime of the Sn(IV) porphycene complexes indicated by the fluorescence quantum yield and lifetime measurement were observed in the case of the Sn(IV) porphycene ([Sn^{IV}(OEPc)Cl_2], $\Phi_F = 0.125$, $\tau_s = 2681$ ps; [Sn^{IV}(OEP)Cl_2], $\Phi_F = 0.010$, $\tau_s = 438$ ps; [Sn^{IV}(OEHPc)Cl_2], $\Phi_F = 0.027$, $\tau_s = 733$ ps). The triplet state of the Sn(IV) complexes was investigated by transient absorption spectroscopy. It became clear that the triplet lifetime of the Sn(IV) porphycene (τ_T = 49.9 μs) was longer when compared to those of the Sn(IV) porphyrin (τ_T = 32.6 μs) and hemiporphycene complexes (τ_T = 28.3 μs). These porphyrin isomer Sn(IV) complexes showed the high singlet oxygen generating ability, and the photo-oxidation of the 1,5-hydroxynaphthalene mediated by the Sn(IV) porphycene was the most effective among the complexes. This result is due to its more effective light absorption in the visible region and indicated that the porphycene is an excellent candidate as a photosensitizer.

Introduction

Porphyrins and phthalocyanines have strong visible absorptions, and they have been attracting much attention, especially because of their potential application as efficient photosensitizers for the photodynamic therapy of cancer.[1,2] Thus, inspired by the significance of the porphyrins, a new research direction has emerged that is devoted to the preparation and study of non-porphyrin tetrapyrrolic macrocycles.[3−5] Recently, many porphyrin isomers with enhanced and unique characteristic properties have been reported.[6] Porphycene and hemiporphycene are some of the artificial tetrapyrrole ligands, and these ligands were first synthesized by Vogel et al.[7−9] It is known that these porphyrin isomers have several interesting properties attributed to their ring-framework modification.[10] These differences have been elucidated from structural, theoretical, and electrochemical studies.[11−16] For example, these porphyrin isomers have a small HOMO−LUMO gap and stronger absorption bands

*To whom correspondence should be addressed. E-mail: yhisatcm@mail.cstm.kyushu-u.ac.jp.

(1) (a) Bonnett, R. *Chem. Soc. Rev.* **1995**, *24*, 19. (b) DeRosa, M. C.; Crutchley, R. J. *Coord. Chem. Rev.* **2002**, *233−234*, 351.
(2) Stockert, J. C.; Cañete, M.; Juarranz, A.; Villanueva, A.; Horobin, R. W.; Borrell, J. I.; Teixido, J.; Nonell, S. *Curr. Med. Chem.* **2007**, *14*, 997.
(3) Shimakoshi, H.; Baba, T.; Iseki, Y.; Endo, A.; Adachi, C.; Hisaeda, Y. *Chem. Commun.* **2008**, 2882.
(4) Baba, T.; Shimakoshi, H.; Endo, A.; Adachi, C.; Hisaeda, Y. *Chem. Lett.* **2008**, *37*, 264.
(5) Shimakoshi, H.; Baba, T.; Iseki, Y.; Endo, A.; Adachi, C.; Watanabe, M.; Hisaeda, Y. *Tetrahedron Lett.* **2008**, *49*, 6198.
(6) Fowler, C. J.; Sessler, J. L.; Lynch, V. M.; Wauluk, J.; Gebauer, A.; Lex, J.; Zuniga-y-Rivero, F.; Vogel, E. *Chem.—Eur. J.* **2002**, *8*, 3485.
(7) Vogel, E.; Köcher, M.; Schmickler, H.; Lex, J. *Angew. Chem., Int. Ed. Engl.* **1986**, *25*, 257.
(8) Vogel, E.; Bröring, M.; Weghorn, S. J.; Scholz, P.; Deponte, R.; Lex, J.; Schmickler, H.; Schaffner, K.; Braslavsky, S. E.; Müller, M.; Pörting, S.; Fowler, C. J.; Sessler, J. L. *Angew. Chem., Int. Ed. Engl.* **1997**, *36*, 1651.
(9) Sánchez-García, D.; Sessler, J. L. *Chem. Soc. Rev.* **2008**, *37*, 215.
(10) (a) Hayashi, T.; Dejima, H.; Matsuo, T.; Sato, H.; Murata, D.; Hisaeda, Y. *J. Am. Chem. Soc.* **2002**, *124*, 11226. (b) Hayashi, T.; Nakashima, Y.; Ito, K.; Ikegami, T.; Aritome, I.; Aoyagi, K.; Ando, T.; Hisaeda, Y. *Inorg. Chem.* **2003**, *42*, 7345. (c) Hayashi, T.; Nakashima, Y.; Ito, K.; Ikegami, T.; Aritome, I.; Hisaeda, Y. *Org. Lett.* **2003**, *5*, 2845. (d) Matsuo, T.; Murata, D.; Hisaeda, Y.; Hori, H.; Hayashi, T. *J. Am. Chem. Soc.* **2007**, *129*, 12906. (e) Ito, K.; Matsuo, T.; Aritome, I.; Hisaeda, Y.; Hayashi, T. *Bull. Chem. Soc. Jpn.* **2008**, *81*, 76. (f) Maeda, D.; Shimakoshi, H.; Abe, M.; Hisaeda, Y. *Dalton Trans.* **2009**, 140. (g) Fujitsuka, M.; Shimakoshi, H.; Tojo, S.; Cheng, L.; Maeda, D.; Hisaeda, Y.; Majima, T. *J. Phys. Chem. A.* **2009**, *113*, 3330.
(11) Nonell, S.; Aramendia, P. F.; Heihoff, K.; Negri, R. M.; Braslavsky, S. E. *J. Phys. Chem.* **1990**, *94*, 5879.
(12) Waluk, J.; Müller, M.; Swiderek, P.; Köcher, M.; Vogel, E.; Hohlneicher, G.; Michl, J. *J. Am. Chem. Soc.* **1991**, *113*, 5511.
(13) Hasegawa, J.; Takata, K.; Miyahara, T.; Neya, S.; Frisch, M. J.; Nakatsuji, H. *J. Phys. Chem. A.* **2005**, *109*, 3187.
(14) Gil, M.; Waluk, J. *J. Am. Chem. Soc.* **2007**, *129*, 1335.
(15) Fita, P.; Radzewicz, C.; Waluk, J. *J. Phys. Chem. A.* **2008**, *112*, 10753.
(16) Fita, P.; Urbańska, N.; Radzewicz, C.; Waluk, J. *Chem. Eur. J.* **2009**, *15*, 4851.

Published on Web 09/23/2009

than those of the porphyrins in the visible region. Therefore, because they are very attractive compounds from a photochemical viewpoint and excellent candidates as photosensitizers,[17] a significant effort has been put into fully characterizing their photochemical properties. Although specific characteristics of porphyrin isomers have been revealed, the photophysical and photochemical properties reflecting the features derived from the ring skeleton change have not been systematically discussed between porphyrin isomers in detail. Therefore, a new insight and knowledge of the photophysical and photochemical properties of the porphyrin isomers are crucial to a better understanding of their functions in various applications.

In the present study, we focused on the influence that a different macrocycle has on the photophysical properties of the porphyrin isomers, and we reported how variations in their electronic structure and nitrogen-core size in the free-base forms of these three systems are reflected in the properties of their corresponding metal complexes, especially focused on the Sn(IV) hemiporphycene and porphycene complexes. As numerous Sn(IV) porphyrins and corroles[18] offer many advantages because of the particular properties conferred by the highly charged main group metal center, they can be possibly used in a variety of applications, that is, in photoinduced electron transfer reactions,[19] in supramolecular chemistry,[20] and as a photocatalyst.[21] Herein, we synthesized the Sn(IV)-porphyrin, hemiporphycene, and porphycene complexes having the same substituent and axial ligands and investigated by several techniques the differences due to the skeleton change. In particular, we compared the photochemical properties of the octaethyl (OE) derivatives in the form of their Sn(IV) complexes (Chart 1).

Experimental Section

Chemicals. For the UV−vis and fluorescent spectroscopy studies, toluene and dichloromethane were purchased from DOJINDO (Japan) and were of spectroscopic grade. For the phosphorescent spectroscopy study, the bromobenzene was purchased from WAKO (Japan) and distilled before use. For the syntheses of **2** and **3**, decahydronaphthalene (decalin) was stirred for 1 day in the presence of sodium metal under a nitrogen atmosphere, then distilled under reduced pressure, and used immediately. The other organic solvents were dried and distilled under a nitrogen atmosphere when necessary.

Chart 1. Chemical Structures of Sn(IV) Complexes **1**, **2**, and **3**

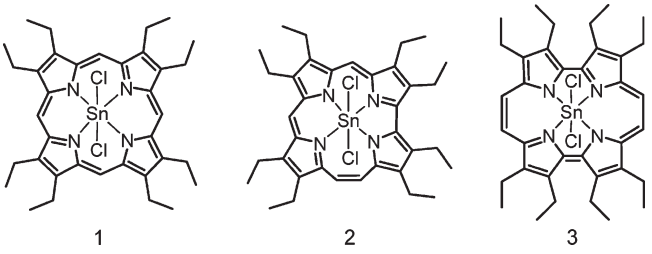

Chart 2. Chemical Structures of Porphyrin, Hemiporphycene, and Porphycene

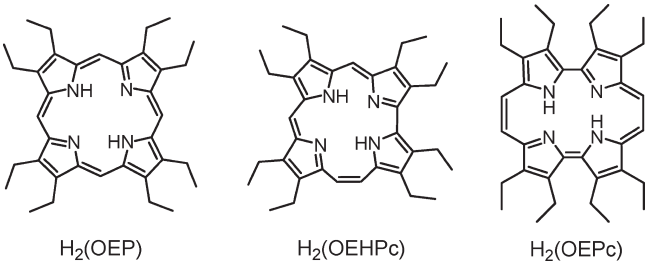

Measurements. The elemental analyses were obtained from the Service Center of Elementary Analysis of Organic Compounds at Kyushu University. The ^{1}H NMR spectra were recorded by a Bruker Avance 500 spectrometer installed at the Center of Advanced Instrumental Analysis at Kyushu University, and the chemical shifts (in ppm) were referenced relative to the residual protic solvent peak. The UV−vis absorption spectra were measured using a Hitachi U-3300 spectrophotometer at room temperature. The fluorescence and phosphorescence spectra were measured by a HORIBA SPEX Fluorolog-NIR spectrophotometer in toluene and bromobenzene at room temperature. Bromobenzene was chosen to readily observe the phosphorescence spectra by the external heavy atom effect. The phosphorescence spectra as shown in this paper are differential spectra of the observed spectra under the anaerobic and aerobic conditions (Supporting Information, Figure S1). The MALDI-TOF mass spectra were obtained using a Bruker Autoflex II without the matrix. The electrospray ionization (ESI) mass spectra were obtained using a JMS-T100CS AccuTOF.

Porphyrin and Porphyrin Isomers. The chemical structures of the porphyrin and porhyrin isomers used in this study are shown in Chart 2. 2,3,6,7,12,13,16,17-Octaethylporphyrin [H_2(OEP)] was purchased from TCI (Japan) and used as received. 2,3,6,7,12,13,16,17-Octaethylhemiporphycene [H_2(OEHPc)] and 2,3,6,7,12,13,16,17-octaethylhemiporphycene [H_2(OEPc)] were synthesized as reported in the literature.[8,22]

Preparation of Sn(IV) Complexes. 2,3,6,7,12,13,16,17-Octaethylporphyrinate Sn(IV) Chloride [Sn^{IV}(OEP)Cl_2] (1). [Sn^{IV}(OEP)-Cl_2] (**1**) was prepared from H_2(OEP) in a manner similar to that previously reported.[23,24] 2,3,6,7,12,13,16,17-Octaethylporphyrin (65 mg, 1.22×10^{-4} mol) and tin(II) chloride dihydrate (260 mg, 1.15×10^{-3} mol) were dissolved in pyridine (10 mL) and refluxed at 115 °C for 2 h. The reaction was monitored by UV−vis spectroscopy until the apparent four-Q bands were transformed into the apparent two-Q bands typical of porphyrin metal complexes. After the reaction solution was evaporated to dryness at

(17) (a) Cañete, M.; Ortiz, A.; Juarranz, A.; Villanueva, A.; Nonell, S.; Borrell, J. I.; Teixido, J.; Stockert, J. C. *Anti-Cancer Drug Des.* **2000**, *15*, 143. (b) Cañete, M.; Lapeña, M.; Juarranz, A.; Vendrell, V.; Borrell, J. I.; Teixidó, J.; Nonell, S.; Villanueva, A. *Anti-Cancer Drug Des.* **1997**, *12*, 543. (c) Villanueva, A.; Cañete, M.; Nonell, S.; Borrell, J. I.; Teixidó, J.; Juarranz, A. *Anti-Cancer Drug Des.* **1996**, *11*, 89. (d) Rubio, N.; Martínez-Junza, V.; Estruga, J.; Borrell, J. I.; Mora, M.; Sagristá, M. L.; Nonell, S. *J. Porphyrins Phthalocyanines* **2009**, *13*, 99.

(18) (a) Walker, D.; Chappel, S.; Mahammed, A.; Brunschwig, B. S.; Winkler, J. R.; Gray, H. B.; Zaban, A.; Gross, Z. *J. Porphyrins Phthalocyanines* **2006**, *10*, 1259. (b) Wagnert, L.; Berg, A.; Stavitski, E.; Berthold, T.; Kothe, G.; Goldberg, I.; Mahammed, A.; Simkhovich, L.; Gross, Z.; Levanon, H. *Appl. Magn. Reson.* **2006**, *30*, 591.

(19) (a) Jang, J. H.; Kim, H. J.; Kim, H.-J.; Kim, C. H.; Joo, T.; Cho, D. W.; Yoon, M. *Bull. Korean Chem. Soc.* **2007**, *28*, 1967. (b) Kim, H. J.; Park, K.-M.; Ahn, T. K.; Kim, S. K.; Kim, S. K.; Kim, D.; Kim, H.-J. *Chem. Commun.* **2004**, 2594.

(20) (a) Slagt, V. F.; van Leeumen, P. W. N. M.; Reek, J. N. H. *Dalton Trans.* **2007**, 2302. (b) Arnold, D. P.; Blok, J. *Coord. Chem. Rev.* **2004**, *248*, 299.

(21) (a) Kim, W.; Park, J.; Jo, H. J.; Kim, H.-J.; Choi, W. *J. Phys. Chem. C.* **2008**, *112*, 491. (b) Monteiro, C. J.; Pereira, M. M.; Azenha, M. E.; Burrows, H. D.; Serpa, C.; Arnaut, L. G.; Tapia, M. J.; Sarakha, M.; Wong-Wah-Chung, P.; Navaratnam, S. *Photochem. Photobiol. Sci.* **2005**, *4*, 617.

(22) (a) Vogel, E.; Koch, P.; Hou, X.; Lex, J.; Lausmann, M.; Kisters, M.; Aukauloo, M. A.; Richard, P.; Guilard, R. *Angew. Chem., Int. Ed. Engl.* **1993**, *32*, 1600. (b) Sessler, J. H.; Hoehner, M. C. *Synlett* **1994**, 211.

(23) Gouterman, M.; Schwart, F. P.; Smith, P. D. *J. Chem. Phys.* **1973**, *59*, 676.

(24) Iwamoto, H.; Hori, K.; Fukazawa, Y. *Tetrahedron* **2006**, *62*, 2789.

room temperature, the residue was extracted with chloroform and washed 2 times with 5% HCl aq. The solution was dried with Na_2SO_4 and evaporated to dryness. The residue was recrystallized in chloroform/cyclohexane and formed violet prism-like crystals (58.8 mg). Yield 67%. UV−vis (in dichloromethane): [λ_{max}/nm] (ε) = 403 (400000); 538 (15300); 575 (14300). Anal. Calcd for $C_{36}H_{44}N_4Cl_2Sn$: C, 59.86; H, 6.14; N, 7.76. Found: C, 59.49; H, 6.00; N, 7.75. TOF-MS (MALDI): m/z [M−Cl]$^+$, 687.23 ([M−Cl]$^+$ calcd for 687.23). ^{1}H NMR ($CDCl_3$, 293 K): δ [ppm] = 2.06 (t, 24H, $-CH_3$), 4.24 (q, 16H, β-CH_2−), 10.59 (s, 4H, −CH−).

2,3,6,7,12,13,16,17-Octaethylhemiporphycenato Sn(IV) Chloride [Sn^{IV}(OEHPc)Cl$_2$] (2). [Sn^{IV}(OEHPc)Cl$_2$] (**2**) was prepared from H_2(OEHPc) in a manner similar to that previously reported.[25] 2,3,6,7,12,13,16,17-Octaethylhemiporphycene (30 mg, 5.61×10^{-5} mol) and tin(II) chloride dihydrate (210 mg, 9.31×10^{-4} mol) were dissolved in dry decalin (36 mL) and refluxed at 200 °C for 0.5 h under a nitrogen atmosphere. The reaction was monitored by UV−vis spectroscopy. The mixture was filtered and then evaporated to dryness in vacuo at room temperature. The residue was purified by column chromatography over neutral silica gel (4 × 15 cm) using dichloromethane/methanol (20:1) as the eluent. The product was then recrystallized from chloroform/cyclohexane to obtain [Sn^{IV}(OEHPc)Cl$_2$] (2) in the form of violet prism-like crystals (32.4 mg). Yield 80%. UV−vis (in dichloromethane): [λ_{max}/nm] (ε) = 391 sh (56800); 416 (231900); 515 (4500); 545 sh (5000); 555 (6600); 587 (37900); 601 (35600). Anal. Calcd for $C_{36}H_{44}N_4Cl_2Sn$: C, 59.86; H, 6.14; N, 7.76. Found: C, 59.34; H, 6.18; N, 7.72. TOF-MS (MALDI): m/z [M−Cl]$^+$, 687.24 ([M−Cl]$^+$ calcd for 687.23). ^{1}H NMR ($CDCl_3$, 293 K): δ [ppm] = 1.99−2.09 (m, 24H, $-CH_3$), 4.20−4.30 (m, 16H, β-CH_2−), 10.47−10.68 (m, 4H, −CH−).

2,3,6,7,12,13,16,17-Octaethylporphycenato Sn(IV) Chloride [Sn^{IV}(OEPc)Cl$_2$] (3). 2,3,6,7,12,13,16,17-Octaethylporphycene (14 mg, 2.61×10^{-5} mol) and tin(II) chloride dihydrate (93 mg, 4.12×10^{-4} mol) were dissolved in dry decalin (18 mL) and refluxed at 200 °C for 0.5 h under a nitrogen atmosphere. The reaction was monitored by UV−vis spectroscopy. The mixture was cooled at room temperature under aerobic conditions and then filtered. The solution was evaporated to dryness under reduced pressure. The residue was extracted with chloroform and washed 2 times with 5% HCl aq. The solution was dried with Na_2SO_4 and evaporated to dryness at room temperature. The residue was recrystallized from chloroform/benzene and formed violet prism-like crystals (17.3 mg). Yield 92%. UV−vis (in dichloromethane): [λ_{max}/nm] (ε) = 377 sh (52000); 400 (141000); 608 (50000); 626 (46000). Anal. Calcd for $C_{36}H_{44}N_4Cl_2Sn$: C, 59.86; H, 6.14; N, 7.76. Found: C, 58.08; H, 5.84; N, 7.42. TOF-MS (MALDI): m/z [M−Cl]$^+$, 687.14 ([M−Cl]$^+$ calcd for 687.23). ^{1}H NMR ($CDCl_3$, 293 K): δ [ppm] = 1.98−2.03 (m, 24H, $-CH_3$), 4.21−4.30 (m, 16H, β-CH_2−), 10.37 (s, 4H, methine).

X-ray Crystallography. All crystals suitable for X-ray analysis were obtained by recrystallization at room temperature. The crystals were mounted on a glass fiber, and used for the X-ray diffraction study. The measurements were made using a Bruker SMART APEX CCD detector with graphite-monochromated Mo Kα radiation (λ = 0.71073 Å) and a 2 kW rotating anode generator. The data were collected at 223 K to a maximum 2θ value of 28.28° in 0.30° oscillations.

The data frames were integrated using SAINT (Version 6.45) and merged to give a unique data set for the structure determination. Empirical absorption corrections by SADABS[26] were carried out. The structure was solved by a direct method, and refined by the full-matrix least-squares method on all F^2 data using the SHELX suite of programs.[27] The non-hydrogen atoms were anisotropically refined. The hydrogen atoms were included in the structure factor calculations, but not refined. As for the complex **2**, it has two elements and the ring structure displays disorder around the central metal, Sn. Thus, an alternative structure is shown in Figure 1b. The crystal data and details of the structure determinations are summarized in Table 1.

Photophysical Measurements. The fluorescence quantum yield (Φ_f) value of **3** was measured using an absolute photoluminescence quantum efficiency measurement system (Hamamatsu C9920-02) incorporating an integrating sphere. To measure the Φ_f, degassed solutions of **3** in toluene were prepared and the concentration was adjusted so that the absorbance of the solution at 337 nm would be less than 0.1. The excitation was performed at 337 nm. In contrast, the determined Φ_f values of **1** and **2** are less than 3% by using this method. In the absolute photoluminescence quantum efficiency measurement, these values are not correct values from the viewpoint of sensitivity. Therefore, the Φ_f values of **1** and **2** were determined by the comparative method of Williams et al. in which 2,7,12,17-tetra-*n*-propyl porphycene was used as the standard.[28] The solutions of the standard and test samples (**1** and **2**) with identical absorbances at the same excitation wavelength can be assumed to be absorbing the same number of photons. Thus, a simple ratio of the integrated fluorescence intensities of both solutions will yield the ratio of the quantum yield values (Supporting Information, Figure S2). To measure Φ_f using this method, degassed solutions of the Sn(IV) complexes (**1** and **2**) in toluene were prepared, and the concentration was also adjusted so that the absorbance of the solution at 337 nm would be 0.1. The excitation was performed at 337 nm.

The transient photoluminescence was measured using a streak camera (Hamamatsu C4780) with a laser diode (LD) (λ = 375 nm, pulse width ∼200 ps, and repetition rate ∼100 MHz) as the excitation source. The fluorescence lifetimes (τ_S) were determined by curve fitting using a microcomputer. The measurement was carried out using a toluene solution under an argon atmosphere.

The transient absorbance spectra were obtained using a laser flash photolysis system (Unisoku TSP-1000M). To measure the transient absorbance spectra, strictly degassed solutions through several freeze−pump−thaw cycles of the Sn(IV) complexes in toluene were prepared, and the concentration was adjusted so that the absorbance of the solution at 355 nm would be 0.4−0.5. A Xe arc lamp was employed as the source of the probe light to follow the spectral changes. For the laser flash photolysis, a sample was excited with 5 ns pulses (355 nm) from a Q-switched Nd:YAG laser (Surelite I, Continuum). The triplet state lifetimes (τ_T) of Sn(IV) complexes were determined by fitting the decay of each triplet−triplet absorption, **1**: 440 nm, **2**: 452 nm, and **3**: 418 nm, respectively. The time course of the absorbance decay was analyzed by single-phase kinetics to determine the lifetimes of the triplet state (τ_T). The rate constant for the oxygen quenching (k_q) was determined from a Stern−Volmer analysis of the triplet lifetime in degassed, air-, and oxygen-saturated solutions as shown in Supporting Information, Figure S3. The measurements for both the air- and oxygen-saturated solutions were performed under similar conditions. The concentration of oxygen for the samples in air (0.0021 M^{-1}) and dioxygen (0.00988 M^{-1}) was used from published oxygen solubility data.[29]

For the singlet oxygen phosphorescence measurements, an air-saturated toluene solution containing the sample in a quartz cell (optical path length 10 mm) was excited at 354 nm using a HORIBA SPEX Fluorolog-NIR at room temperature. Each singlet oxygen quantum yield (Φ_Δ) value (**1**−**3**) was determined

(25) Scholz, P. J. Ph.D. Thesis, University of Köln, Köln, Germany, **1998**.
(26) Sheldrick, G. M. *SADABS*; University of Göttingen: Göttingen, Germany, 1996.
(27) Sheldrick, G. M. *SHELXL97 and SHELXS97*; University of Göttingen: Göttingen, Germany, 1997.
(28) Williams, A. T. R.; Winfield, S. A.; Miller, J. N. *Analyst* **1983**, *108*, 1067–1071.
(29) Montalti, M.; Credi, A.; Prodi, L.; Gandolfi, M. T. *Handbook of Photochemistry*, 3rd ed.; CRC Press: Boca Raton, FL, 2006.

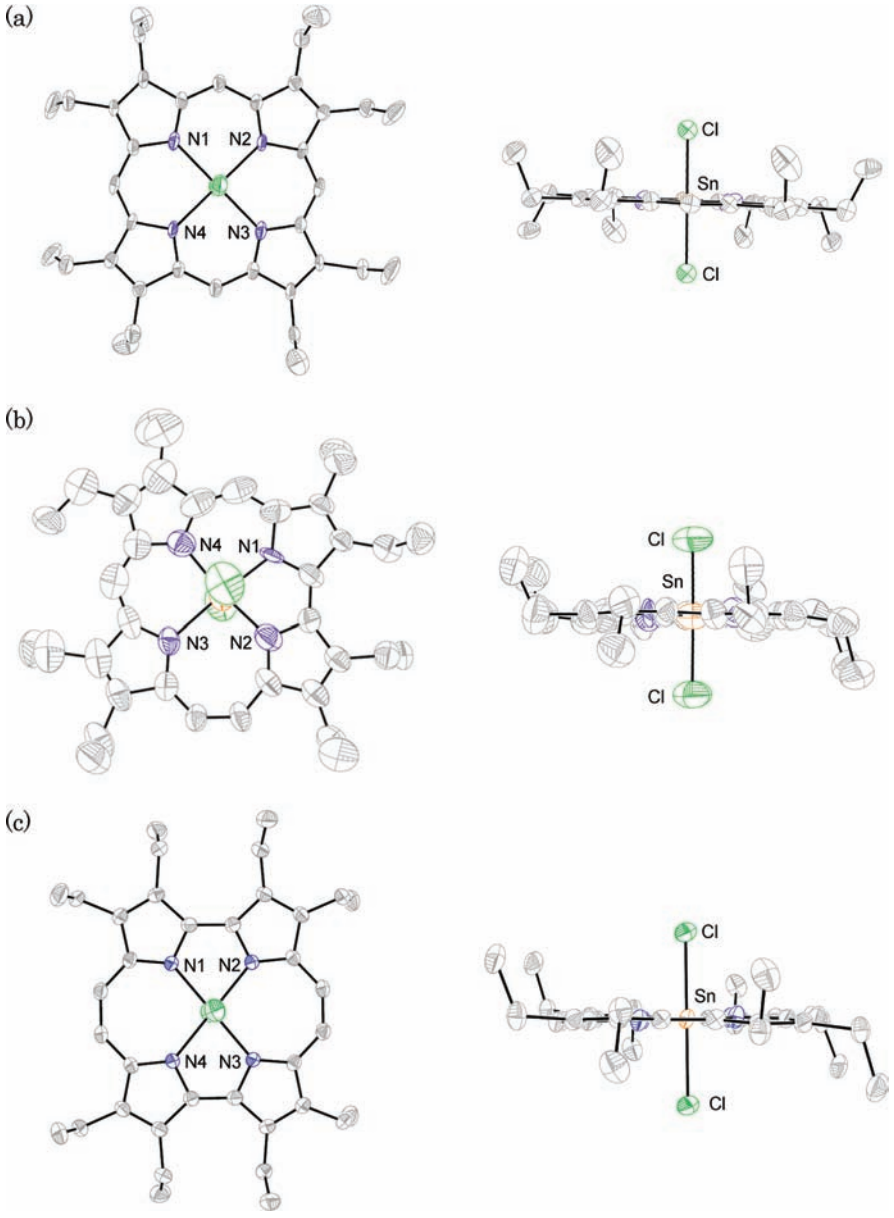

Figure 1. ORTEP drawing of Sn(IV) complexes (a) **1**, (b) **2**, and (c) **3** with thermal ellipsoids at 50% probability. Hydrogen atoms and the crystallization solvents have been omitted for clarity.

from the slope of the plot with an intensity at 1270 nm versus the concentrations of the Sn(IV) complexes based on 2,7,12,17-tetra-*n*-propyl porphycene as the standard ($\Phi_\Delta = 0.36$) as shown in Supporting Information, Figure S4.

Catalytic Reaction. The catalytic photo-oxygenation of 1,5-dihyroxynaphthalene was investigated under aerobic conditions at room temperature: ([sensitizer] = 1.0 μM, [substrate] = 3.33 mM, solv. CH_2Cl_2-MeOH (9: 1 v/v)). These reaction solutions were stirred during irradiation by a 500 W tungsten-lamp through a cutoff filter (TOSHIBA Y-46, >460 nm). The progress of the reaction was monitored by absorption at 427 nm, typical for the product, 5-hydroxy-1,4-naphthoquinone (Juglone). The product was isolated and identified according to previous method.[3,5] ^{1}H NMR ($CDCl_3$, 293 K): δ [ppm] = 6.94 (s, 2H), 7.27 (dd, 1H), 7.60−7.65 (m, 2H), 11.90 (s, 1H, OH), GC-MS (EI): m/z = 174 (M^+).

Results and Discussion

Syntheses and Structural Studies of Sn(IV) Complexes. The Sn(IV)-dichloro complexes, **1**, **2**, and **3**, were obtained by treatment of the free base ligands with tin(II) chloride dehydrate in a high-boiling solvent, such as pyridine or decalin. The reactions were monitored by UV−vis spectroscopy until the apparent three or four-Q bands are transformed into the apparent two-Q bands typical of porphyrin and porphyrin isomer metal complexes.[23] The obtained complexes were characterized by UV−vis, ^{1}H NMR, and mass spectroscopies, and the crystal structures were determined by X-ray analysis. These complexes show a parent ion resulting from the loss of one chloro ligand under the MALDI-TOF mass spectral analysis conditions. All the Sn(IV) complexes suitable for X-ray analysis were obtained by recrystallization at room temperature. The crystal structure of the porphyrin complex, **1**, has already been reported,[30] but the crystal structure with chloroform as the solvent is a new one.

(30) (a) Cullen, D. L.; Meyer, E. F. *Chem. Commun.* **1971**, 616. (b) Cullen, D. L.; Meyer, E. F. *Acta Crystallogr.* **1973**, *B29*, 2507.

Table 1. Crystallographic Data for **1**, **2**, and **3**

parameter	**1**	**2**	**3**
formula	$C_{37}H_{45}N_4SnCl_5$	$C_{36}H_{44}N_4SnCl_2$	$C_{36}H_{44}N_4SnCl_2$
formula weight	841.71	722.34	722.34
crystal system	monoclinic	monoclinic	monoclinic
space group	$P2(1)/n$	$P21$	$P2(1)/c$
a/Å	8.208(2)	8.4442(15)	8.2024(10)
b/Å	17.645(5)	13.808(3)	13.9702(16)
c/Å	15.195(5)	14.573(3)	14.3172(17)
β/deg	105.633(6)°	97.748(3)°	100.202(3)°
V/Å^3	2119.4(11)	1683.7(5)	1614.7(3)
Z	2	2	2
T/K	223(2)	223(3)	223(3)
ρ_{calc}/g cm^{-3}	1.391	1.425	1.486
μ/mm^{-1}	0.947	0.949	0.989
reflections measured	10333	9777	7906
unique reflections	3058	5851	2304
R_{int}	0.0718	0.0280	0.0225
observed data [$I > 2\sigma(I)$]	2510	3308	2032
$R1$ [a] wR_2 [b] [$I > 2\sigma(I)$]	0.0723, 0.1817	0.0716, 0.1904	0.0236, 0.0637
$R1$ [a] wR_2 [b] (all data)	0.0877, 0.1926	0.1223, 0.2430	0.0269, 0.0670

[a] $R1 = \sum||F_o| - |F_c||/\sum|F_o|$. [b] $wR_2 = [\sum w(F_o^2 - F_c^2)^2/\sum w(F_o^2)^2]^{1/2}$.

Table 2. Bond Lengths (Å) and Bond Angles (deg) of **1**, **2**, and **3**

			1		
Sn−Cl	2.463	N1−N2	2.941	N1−Sn−N2	89.81
Sn−N1	2.079	N2−N3	2.950	N2−Sn−N3	90.19
Sn−N2	2.087	N3−N4	2.941	N3−Sn−N4	89.81
Sn−N3	2.079	N1−N4	2.950	N1−Sn−N4	90.19
Sn−N4	2.087				
			2		
Sn−Cl	2.441	N1−N2	2.593	N1−Sn−N2	81.49
Sn−N1	1.990	N2−N3	3.119	N2−Sn−N3	93.96
Sn−N2	1.987	N3−N4	3.086	N3−Sn−N4	92.16
Sn−N3	2.230	N1−N4	2.881	N1−Sn−N4	91.00
Sn−N4	2.049				
			3		
Sn−Cl	2.462	N1−N2	2.630	N1−Sn−N2	79.02
Sn−N1	2.068	N2−N3	3.189	N2−Sn−N3	100.98
Sn−N2	2.065	N3−N4	2.630	N3−Sn−N4	79.02
Sn−N3	2.068	N1−N4	3.189	N1−Sn−N4	100.98
Sn−N4	2.065				

Moreover, the X-ray crystal structure of the Sn(IV) complexes with porphycene and hemiporphycene have not been revealed and are the first examples of an X-ray analysis. The X-ray crystal structures of these complexes, **1**, **2**, and **3**, are shown in Figure 1. The central metal Sn for all the complexes coordinates with the N4 core and has dichloride ions as the axial ligands.

Table 2 lists the parameters for the coordination environments of the Sn(IV) complexes, **1**, **2**, and **3**. Comparison of all the Sn(IV) complexes show many similarities but some striking differences. For example, the central Sn ion is displaced in the mean plane of the four coordination pyrrole N atoms, but these core shapes are different (**1**: square, **2**: quadrilateral, and **3**: rectangular). Furthermore, the bond length of Sn−Cl (2.463 Å) in **1** is slightly longer than those of **2** (2.441 Å) and **3** (2.462 Å). This is presumably attributed to the average Sn−N distances (**1**: 2.083 Å; **2**: 2.064 Å; **3**: 2.067 Å). Therefore, the interaction between the central Sn and the chloride ion may be weaker in **1** compared to those in **2** and **3**.

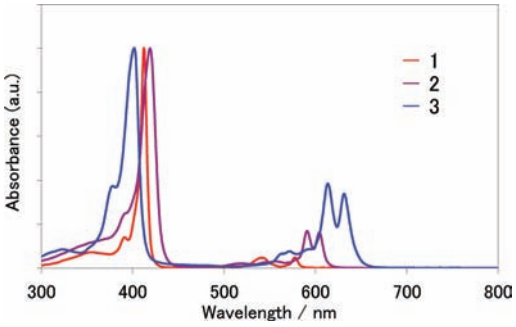

Figure 2. UV−vis spectra of **1**, **2**, and **3** normalized at each Soret band in toluene.

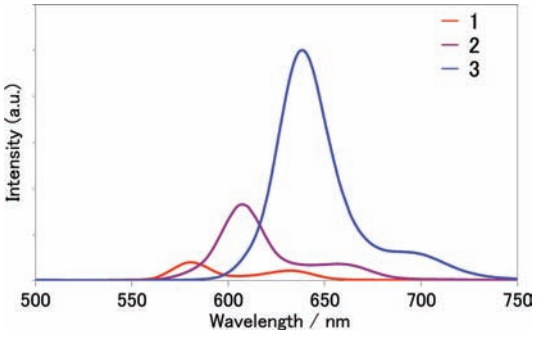

Figure 3. Fluorescence spectra for **1**, **2**, and **3** in toluene. The optical densities of all samples are adjusted to be the same at the excitation wavelength of 400 nm (Abs. = 0.5).

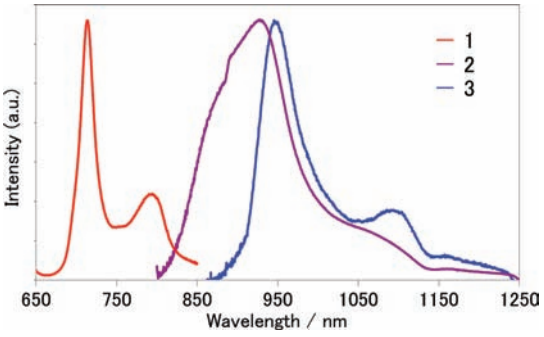

Figure 4. Phosphorescence spectra for **1**, **2**, and **3** in bromobenzene.

Spectroscopic Properties of Sn(IV) Complexes. Figure 2 shows the absorption spectra of **1**, **2**, and **3** in toluene. These complexes have characteristic absorption bands around 400 nm derived from the Soret band and around 600 nm due to the Q-band with large extinction coefficients (ε). In particular, the porphycene Sn(IV) complex **3** exhibits extraordinary large absorption bands ($\varepsilon \approx$ 100000) for the Q-band compared to the other Sn(IV) complexes, **1** and **2**. Also, the absorption bands in the visible region are red-shifted in the order **1**, **2**, and **3**. In general, it is known that the absorption band of porphyrin and porphyrin isomers are mainly raised from $\pi-\pi^*$ transitions of the macrocycle.[13] Thus, the red-shifted Q-band of **2** and **3** are caused by significant stabilization of the lowest unoccupied molecular orbital (LUMO) energy level with a decrease in the symmetry of the tetrapyrrolic macromolecule.

Table 3. Spectroscopic Data of Sn(IV) Complexes[a]

compound	λ_{abs}[b]/nm (10^{-4} ε/M $^{-1}$cm^{-1})	λ_{fluo}[c]/nm	Φ_F[c,d]	τ_S[c]/ps	λ_{phos}[e]/nm	E_S[f]/kJ mol^{-1}	E_T /kJ mol^{-1}
1	403(40.0), 538(1.53), 575(1.43)	580.6	0.010	438 (100%)	713.5	207.4	167.6
2	416(23.2), 587(3.79), 601(3.56)	604.5	0.027	733 (100%)	927.0	198.5	129.0
3	400(25.0), 608(9.10), 626(8.50)	631.5	0.125	2681 (100%)	945.5	190.6	126.5

[a] λ_{abs}: absorption maximum; λ_{fluo}: fluorescence maximum; λ_{phos}: phosphorescence maximum; E_S: lowest excited singlet energies; E_T: lowest excited triplet energies. [b] Solvent, dichloromethane. [c] Solvent, toluene. [d] The absolute fluorescence quantum yield value was based on photoluminescent measurements using an integrating sphere with excitation wavelength at 337 nm. [e] Solvent, bromobenzene degassed in vacuo. [f] The singlet energy was estimated from the intersection point of the normalized absorption and fluorescence spectra.

As shown in Figure 3, the relatively strong emissions for **1**, **2**, and **3** are exhibited by an excitation wavelength at 400 nm in toluene, and their fluorescence intensities are significantly influenced by a difference of the ring structure. Also, the phosphorescence bands in the near-infrared region are red-shifted in the order **1**, **2**, and **3** for similar reasons (Figure 4). The fluorescence quantum yield (Φ_F) and singlet lifetime (τ_S) of the Sn(IV) complexes are summarized in Table 3. Complex **3** shows a fluorescence with a maximum at 631.5 nm and quantum yield of Φ_F = 0.125 in an argon-saturated solution. This value is significantly higher than that of H_2(OEPc) (Φ_F = 0.017).[8] It is proposed that the internal conversion of the excited state is accelerated by the steric repulsion of the ethyl group at the pyrrole β-position of the H_2(OEPc). Thus, it is attributed to the fact that metalation flattened the ring skeleton of **3**, and the internal conversion was inhibited.

When the fluorescence lifetimes (τ_S) were measured in the same solutions, the porphycene Sn(IV) complex **3** showed a very long lifetime (2681 ps) compared to those of the other complexes (**1**: 438 ps, **2**: 733 ps). The fluorescence rate constant (k_f) were readily calculated as $k_f = \Phi_F/\tau_S$ using the measured values. As a result, there is a slight difference in k_f for Sn(IV) complexes (**1**: 2.3×10^7, **2**: 3.7×10^7, **3**: 4.7×10^7 s^{-1}, respectively). This is consistent with the higher molar absorption coefficient (Strickler−Berg equation).[31] Moreover, it is expected that the internal conversion rate constants (k_{ic}) are almost the same values based on the energy-gap law because their singlet energies are slightly different (207.4, 198.5, and 190.6 kJ mol^{-1}, respectively).[32] It is thus conceivable that the intersystem crossing rate constant (k_{isc}) of **3** is critically slower than those of **1** and **2**. Therefore, the fluorescence lifetime (2681 ps) of **3** is quite long by comparison with that of the other complexes. Similar trends in the excited state are observed in the case of [Sn(TPrPc)Cl_2], in which TPrPc denotes the 2,7,12,17-tetra-*n*-propyl porphycene ligand.[33] Therefore, these spectroscopic measurements lead to the suggestion that the long fluorescence lifetime and the slow intersystem crossing rate constant are specific properties of the metalloporphycene.

Triplet Lifetime (τ_T) of Sn(IV) Complexes and Reactivity with Molecular Oxygen. The photophysical property data, in particular, the triplet state of the porphyrin, hemiporphycene, and porphycene complexes, are important to understand the influence derived from a different macrocycle. The transient absorption spectra for Sn(IV) complexes were obtained by laser flash photolysis, and show common bands around 400−450 nm derived from the triplet−triplet absorption bands (Supporting Information, Figure S5). The triplet lifetimes of the Sn(IV) complexes were determined by fitting the decay of the triplet−triplet absorption excited at 355 nm (Abs. = 0.5).

Table 4 lists the values obtained for the triplet lifetimes and oxygen quenching rate constants (k_q), which were calculated from a Stern−Volmer analysis of the triplet lifetime in aerated, deaerated, and oxygen-saturated solutions (Supporting Information, Figure S4). The triplet state of **3** is 49.9 μs in a deaerated solution, much longer than those of **1** (τ_T = 32.6 μs) or **2** (τ_T = 28.3 μs). This result is the sum of the non-radiative decay and phosphorescence rate constant (**1**: 4.81×10^4, **2**: 4.75×10^4, and **3**: 0.14×10^4 s^{-1}, respectively). Thus, it presumably suggested that the spin-inversion process from the triplet state to the ground state is slower than those of **1** and **2** similar to the intersystem crossing process. In contrast, the oxygen quenching rate constant (k_q) of **3** is slightly

Table 4. Triplet Lifetimes (τ_T) in Aerated and Deaerated Solutions with Respective Oxygen Quenching Rate Constants (k_q), and Singlet Oxygen Quantum Yield (Φ_Δ)[a]

compound	τ_{O2}/ns	τ_{N2}/μs	$k_q(O_2)$/ M^{-1} s^{-1}	$k_p + k_{nr}$/s^{-1}	Φ_Δ[b]	$P^T{}_{O2}$[c]
1	82.1	32.6	1.23×10^9	4.81×10^4	0.925	0.982
2	72.8	28.3	1.39×10^9	4.75×10^4	0.971	0.984
3	52.8	49.9	1.92×10^9	0.14×10^4	0.673	0.999

[a] Solvent, toluene. [b] The quantum yield for singlet oxygen generation was relatively determined using TPrPc as standard (λ_{ex} = 354 nm, Φ_Δ = 0.36). [c] The quenching efficiency by molecular oxygen for the excited triplet state.

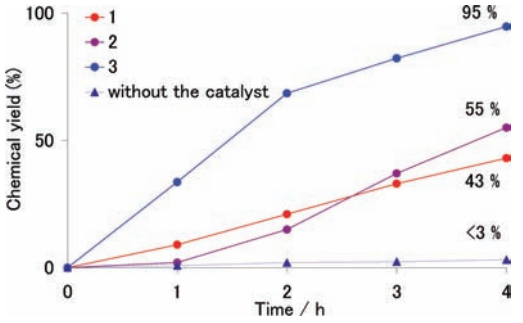

Figure 5. Photoirradiation time profile of the photo-oxygenation of 1,5-dihydroxynaphthalene (3.33 mM) in the presence of photosensitizer (1.0 μM) in CH_2Cl_2-MeOH (9: 1 v/v) in air at room temperature.

(31) Rubio, N.; Prat, F.; Bou, N.; Borrell, J. I.; Teixido, J.; Villanueva, A.; Juarranz, A.; Cañete, M.; Stockert, J. C.; Nonell, S. *New J. Chem.* **2005**, *29*, 378.

(32) Englman, R.; Jortner, J. *J. Lumin.* **1970**, *1*−*2*, 134.

(33) [Sn(TPrPc)Cl_2] was prepared in a manner similar to that of [Sn(OEPc)Cl_2]. UV−vis (in dichloromethane): [λ_{max}/nm](ε) 391 (134000); 404 (125000); 606 (54000); 625 (89000). Anal. Calcd for $C_{36}H_{44}N_4Cl_2Sn$: C, 57.69; H, 5.45; N, 8.41. Found: C, 57.58; H, 5.41; N, 8.38. The fluorescence quantum yield (Φ_F) and lifetime (τ_s) were measured using the same methods: Φ_F = 0.092, τ_s = 3397 (98%), 9720 (2%) ps.

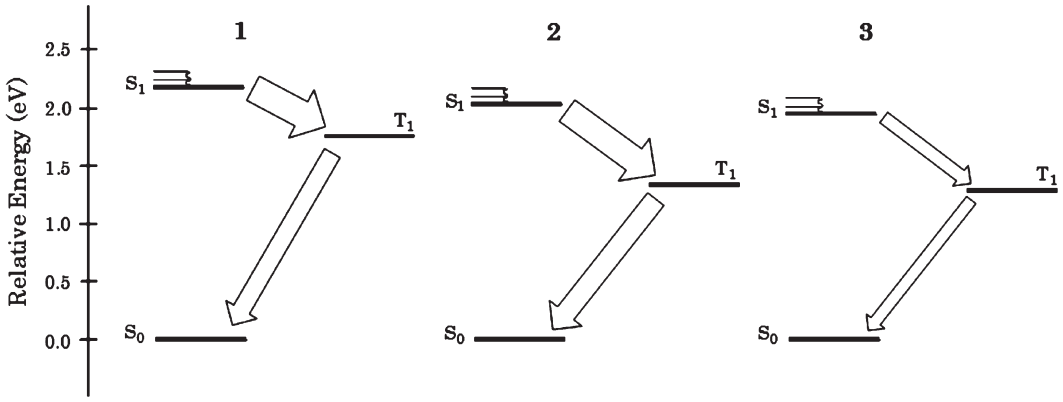

Figure 6. Approximate energy-level diagram and schematic representation for the Sn(IV) complexes **1**, **2**, and **3** based on UV−vis absorption, emission, and lifetime data of singlet and triplet state. The size of the arrow represents the probable rate of spin-inversion processes (S_1-T_1, T_1-S_0).

Scheme 1. Catalytic Photo-oxygenation of 1,5-Dihyroxynaphthalene by the Singlet Oxygen in Air at Room Temperature

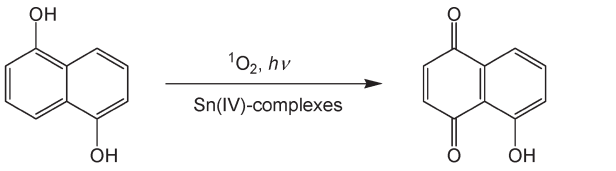

1,5-dihyroxynaphthalene 5-hydroxy-1,4-naphthoquinone

higher by comparison with **1** and **2**. It is known that sensitizers should have a triplet state of appropriate energy ($E_T \geq 95$ kJ mol^{-1}) to allow for efficient energy transfer to the ground state oxygen.[1] It was reported that the rate constant of the energy transfer to the ground state oxygen depends on the energy of the triplet state. Thus, the rate of energy transfer is fast enough so that the energy gap between the triplet state of the sensitizer and the singlet state of oxygen is small.[34] Therefore, the respective oxygen quenching rate constants are reflected in the E_T values for the Sn(IV) complexes.

The singlet oxygen generating ability of a photosensitizer is evaluated by its quantum yield (Φ_Δ). The singlet oxygen quantum yields (Φ_Δ) following laser excitation of the sensitizer solutions can be obtained from a comparison of the singlet oxygen phosphorescence intensity at 1270 nm with that of an optically matched reference sensitizer. In the present study, the Φ_Δ values of the Sn(IV) complexes were determined from 2,7,12,17-tetra-*n*-propyl porphycene (TPrPc) as the standard (Φ_Δ = 0.36).[35] These singlet oxygen quantum yields (Φ_Δ) are summarized in Table 4.

The singlet oxygen production ability of the Sn(IV) complexes are enhanced by the internal heavy-atom effect, and the highest value of 0.97 for its quantum yield (Φ_Δ) was obtained for the Sn(IV) hemiporphycene complex, **2**. On the other hand, the Sn(IV) porphycene complex, **3** showed a lower quantum yield value (Φ_Δ = 0.67) than those for the other Sn(IV) complexes. As described above, this result is attributed to the fact that the intersystem-crossing rate of **3** is much slower than those of the other complexes. However, the quenching efficiency (P^T_{O2}) by molecular oxygen for the excited triplet state of **3** is quite high at about 1. Therefore, the Sn(IV) porphycene complex **3** is an attractive compound and excellent candidate as a photosensitizer because of its extraordinary large absorption bands ($\varepsilon \approx 100000$) in the visible region.

Photoreaction Catalyzed by a Sensitizer. The catalytic photo-oxygenation of 1,5-dihydroxynaphthalene was investigated as shown in Scheme 1. The reaction was monitored by absorption at 427 nm, typical for the product, 5-hydroxy-1,4-naphthoquinone (Juglone, ε = 3370).[36] The reaction of singlet oxygen resulted in the quantitative conversion of 1,5-dihyroxynaphthalene to 5-hydroxy-1,4-naphthoquinone. And also, the catalyst bleaching of these Sn(IV) complexes were not observed during the reaction. The respective chemical yields of the product are shown in Figure 5. In the case of **3**, the photoreaction most effectively proceeded, and the substrate was completely converted to the oxygenated product in 4 h. As summarized in Table 4, the higher values of 0.97 and 0.93 for its Φ_Δ are obtained for **1** and **2**, respectively. In contrast, **3** showed a lower quantum yield value (Φ_Δ = 0.67) than those for the other complexes. Nevertheless, the Sn(IV) porphycene complex **3** showed very high chemical yields. This result is caused by an extraordinary large absorption band of **3** in the visible region. Thus, the advantage of the porphycene over porphyrin and hemiporphycene in the photoreaction is due to its more effective light absorption in the visible region.

Conclusion

A new insight into the photophysical and photochemical properties of the porphyrin isomers is crucial to better understand their function during various photoreactions. In this study, the Sn(IV)-porphyrin, hemiporphycene, and porphycene complexes with analogous skeletons were synthesized, and the differences in their photochemical and photophysical properties due to the skeleton change were compared in detail. It became clear that there is a considerable difference between the singlet (S_1) and the triplet (T_1)

(34) (a) Ozoemena, K.; Kuznetsova, N.; Nyokong, T. *J. Mol. Catal. A* **2001**, *176*, 29. (b) Engelmann, F. M.; Mayer, I.; Araki, K.; Toma, H. E.; Baptista, M. S.; Maeda, H.; Osuka, A.; Furuta, H. *J. Photochem. Photobiol. A* **2004**, *163*, 403.

(35) (a) Redmond, R. W.; Valduga, G.; Nonell, S.; Braslavsky, S. E.; Schaffner, K.; Vogel, E.; Pramod, K.; Köcher, M. *J. Photochem. Photobiol. B* **1989**, *3*, 193. (b) Aramendia, P. F.; Redmond, R. W.; Nonell, S.; Schuster, W.; Braslavsky, S. E.; Schaffner, K.; Vogel, E. *Photochem. Photobiol.* **1986**, *44*, 555.

(36) Suchard, O.; Kane, R.; Roe, B. J.; Zimmermann, E.; Jung, C.; Waske, P. A.; Mattay, J.; Oelgemöller, M. *Tetrahedron* **2006**, *62*, 1467.

states of **3** and the other complexes, although the spin-inversion processes (S_1-T_1, T_1-S_0) are enhanced by the internal heavy-atom effect of the central Sn metal. The long fluorescence (τ_S), the triplet (τ_T) lifetime, and relatively small singlet oxygen quantum yield (Φ_Δ) of **3** compared to those of the other complexes are attributed to the porphycene skeleton. Therefore, these results suggested that the heavy-atom influence on the spin-inversion processes of porphycene is mildly effective in comparison to those of the porphyrin and hemiporphycene as shown in Figure 6. Thus, the spin-inversion processes in **3** could be slower than those of **1** and **2**. However, porphycene has an advantage in the photoreaction because of its more effective light absorption in the visible region and thus is an excellent candidate as a photosensitizer.

Acknowledgment. We are grateful to Prof. E. Vogel of Köln University for a gift of a sample of H_2(OEHPc) and useful information. We thank Prof. K. Sakai and Dr. S. Masaoka of Kyushu University for helping to measure the transient absorption spectra, Prof. C. Adachi and Mr. A. Endo of Kyushu University for helping to measure the fluorescence quantum yield and lifetime. This study was supported by a Grant-in-Aid for Scientific Research on Priority Areas (No. 460, "Chemistry of Concerto Catalysis"), the Global COE Program "Science for Future Molecular System" from the Ministry of Education, Culture, Sports, Science and Technology of Japan (MEXT), the a Grant-in-Aid for Scientific Research (20.02314) and a Grant-in-Aid for Scientific Research (A) (No. 21245016) from the Japan Society for the Promotion of Science (JSPS).

Supporting Information Available: The crystallographic data in CIF format and experimental details. This material is available free of charge via the Internet at http://pubs.acs.org.